Thin-Walled Structures 95 (2015) 183–195

Contents lists available at ScienceDirect

Thin-Walled Structures

journal homepage: www.elsevier.com/locate/tws

A penalty approach to obtain lower bound buckling loads for imperfection-sensitive shells

Luis A. Godoy [a,b,*], Rossana C. Jaca [c], Eduardo M. Sosa [d], Fernando G. Flores [a,b]

[a] Institute for Advanced Studies in Engineering and Technology, CONICET-UNC, Argentina
[b] Departamento de Estructuras, FCEFyN, Universidad Nacional de Córdoba, P.O. Box 916, Córdoba, Argentina
[c] Civil Engineering Department, Facultad de Ingeniería, Universidad Nacional del Comahue, Buenos Aires 1400, Neuquén, Argentina
[d] Civil and Environmental Engineering Department, West Virginia University, Morgantown, WV 26506-6103, USA

ARTICLE INFO

Article history:
Received 12 June 2015
Received in revised form
3 July 2015
Accepted 5 July 2015

Keywords:
Buckling
Finite elements
Reduced energy method
Perturbation methods
Stability
Shells

ABSTRACT

The strategy of Reduced Stiffness (or Reduced Energy) Analysis, in which selected energy components are eliminated to account for mode interaction and imperfection-sensitivity in a simplified way, was developed by Croll and co-workers since the early 1980s. This physical interpretation allows the formulation as an eigenvalue problem, in which the eigenvalue (critical load) is a lower bound to experiments and to nonlinear incremental analysis. This paper considers the computational implementation of both reduced stiffness and reduced energy approaches to the buckling of shell structures by means of perturbation techniques and penalty parameter methods. The structural configurations of interest in this work are cylindrical shells with or without a roof. The reduced stiffness approach has been implemented in a special purpose finite element code for shells of revolution, whereas the reduced energy methodology was implemented in a general purpose finite element code. The present results are compared with geometrically nonlinear analysis including geometric imperfections. Achievements and difficulties in extending the methodologies to complex problems in engineering practice are highlighted.

1. Introduction

Attempts have been made by researchers to develop simple computational tools to provide approximate solutions to shell buckling problems and avoid gross errors in solutions without the need that the user has knowledge of the complete arsenal of shell buckling theory. James G.A. Croll promoted the use of a simple technique based on a reduced version of the energy (or the stiffness) of the shell, in which only an eingen-value problem needs to be solved. This paper discusses ways to implement such methodology in more complex engineering problems using finite element codes.

The European approach to the analysis of shell buckling problems [1] using finite element tools identifies several possible types of analysis, including Geometrically and Material Nonlinear Analysis with Imperfections (GMNIA) as the "best" estimate of buckling capacity; Geometric Nonlinear Analysis with Imperfections (GNIA); Material Nonlinear Analysis (MNA); and Linear Bifurcation Analysis (LBA). An intermediate method is recommended as a "less onerous" approach, which is based on a combination of LBA and MNA. The recommended approach requires design curves that need to be established for each geometric and load configuration, which take the form of elasto-plastic interaction curves. The parameters of such curves should be obtained from a number of full GMNIA, and once the curves are constructed for a specific class they can be used by performing LBA and MNA studies for a given case of interest. The non-specialist engineer who does not have the curves for his/her own problem is therefore lost since the start. A specialist engineer, on the other hand, needs to spend time and effort to develop the tools before using them.

In the American approach the loads are specified, such as in the ASCE provisions [3], but the engineer is left to decide what type of analysis is suited for each case. Of course, this is a job for the specialist engineer, because a novice may mix concepts and approaches to yield incorrect solutions.

The question of what is "onerous" in computational mechanics, as is the concern of the European Committee for shell buckling [1], has considerably changed over the last decades. In 2015 the "onerous" part of the job consists in understanding the physics of the problem and conceptually modeling the case in hand.

* Corresponding author.
E-mail addresses: lgodoy@efn.uncor.edu (L.A. Godoy), rossana.jaca@fain.uncoma.edu.ar (R.C. Jaca), eduardo.sosa@mail.wvu.edu (E.M. Sosa), fflores@efn.uncor.edu (F.G. Flores).

http://dx.doi.org/10.1016/j.tws.2015.07.005
0263-8231/

We shall not refer here to shell buckling problems in general terms, but attention will be restricted to very thin shells, with radius to thickness slenderness between 1000 and 2000, such as those employed in the fabrication of storage tanks for the oil industry, which tend to buckle in the elastic range and plasticity develops only in advanced post-buckling states. There are also functional requirements that need to be considered, as in any case in industry: storage tanks usually have an internal floating roof that floats on top of the oil or fuel, and large buckling deflections may be sufficient to block the floating mechanism, with the consequence that the structure has to be left out-of-service until it is repaired.

Regarding the nature of imperfections, one may distinguish between global imperfections (possibly due to errors in fabrication or damage under previous loads) and local imperfections (such as welding defects). Following Koiter's asymptotic formulation [2], in the vicinity of a critical state the most detrimental shape of imperfection is the eigenmode associated with the lowest eigenvalue (this is called an eigenmode-affine imperfection). Because Koiter employed an asymptotic approach centered on a bifurcation point, the validity of his results is limited to small post-buckling displacements and small imperfection amplitudes; this however allows comparisons to be made between different shapes of imperfections. For a number of years, imperfections were almost exclusively assumed in the form of an eigenmode-affine imperfection.

The choice of this shape of imperfection has also been emphasized in the European Recommendations in statements like: "The eigenmodes affine pattern is the critical buckling mode associated with the elastic critical buckling resistance based on an LBA analysis of the perfect shell" ([1], pp. 125).

The research program known as lower bound buckling based on Reduced Stiffness/Reduced Energy Analysis (abbreviated in this paper as RSA and REA, respectively), developed in stages over a period starting in the mid-seventies. A summary of the main contributions is next presented, to highlight the research achievements made during the past 45 years.

The first stage was establishing the physics of the problem and the basis of the methodology. Croll discussed the first account of the lower bound approach, largely based on physical observations on the buckling of imperfection-sensitive shells, as follows: "It is shown that the highly unstable forms of buckling involve essentially a process in which the significant membrane contribution to resistance against incremental displacement at the initial stages of buckling is transferred in the advanced post-buckling states to a situation in which bending energy tends to dominate in providing the resistance to incremental displacements" [4]. This first approach involved some speculation concerning the nonlinear process that occurs at the passage to post-buckling states in cylinders under axial loads.

The first systematic approach for cylinders under lateral pressure was based on analytical studies reported by Batista and Croll. Based on physical reasoning, the authors argued that "the unstable post-critical behavior is the result of the loss of this membrane stiffness" [5]. A simplified methodology was presented in which "appropriate terms in the membrane potential energy are neglected". The results were supported by experiments performed by the authors and were shown to provide a lower bound to experiments of other authors as well. The extension of this methodology to axially loaded cylinders was published a few years later [6].

A second stage was the extension of the methodology to other cylindrical shell configurations, namely stiffened cylinders. Emphasis shifted from understanding the physics of the problem to providing a design methodology, thus addressing more complex shell configurations usually found in off-shore structures and providing simple expressions which could be used in design. Thus, the research program addressed elastic buckling of stringer [7,8] and ring stiffened cylinders [9,10], and combination of ring and stringer stiffeners [11].

Extensions of the lower bound approach to shell configurations other than cylinders were pioneered by Zintillis and Croll in a series of papers on cooling towers under wind or lateral pressure. Following an analysis of the energy components, the reduced stiffness critical spectrum was obtained by suppressing the membrane strain energy U^{2m} from the classical analysis, leading to a reduced critical load

$$\lambda^* = \frac{U^{2b}}{U^{2m} + U^{2b}}\lambda^C \tag{1}$$

where U^{2b} is the bending energy contribution [12]. This computational research was supported by experiments on toroidal and hyperboloidal shells. This was the first analysis performed using a finite element special purpose code to model the shell, and the code was limited to axisymmetric loading. Analysis for combined axial and lateral loading was reported in [13]. For wind-loaded shells, the worst stressed meridian approach was employed thus assuming the equivalence between the asymmetric wind pressure and a symmetric pressure. Uniform thickness was employed in all cases [14]. Pressure-loaded spherical caps were addressed by Goncalves and Croll [15], whereas Kashani and Croll [16] investigated spherical space domes. Other researchers employed the methodology for composite materials [17,18], and this interest has recently been extended to aeronautical applications [19].

A third stage involved the extensions of the methodology to account for elasto-plastic buckling of cylinders. This was done with simple analytical expressions and was reported in Refs. [20–23].

A fourth stage was the computation of nonlinear analyses, which were performed analytically by Yamada and Croll [24–26] using a nonlinear Ritz analysis.

The best readings reviewing the lower bound approach were presented by Croll as a design methodology [27,28] in which details of the motivations and achievements at each stage are discussed in an amenable way.

In summary, the RSA/REA studies by Croll and co-workers were based on

- Analytical methods to obtain explicit expressions for lower bound buckling loads which could be used in design. Use of finite element models was the exception in the work of Zintillis, because explicit expressions could not be found for the configurations of interest.
- Shells with uniform thickness were addressed. Although this may be seen as a trivial simplification in real cases, modeling thickness changes brings some additional difficulties to the application of RSA or REA.
- Shells considered were subjected to axi-symmetric loads (either axial or lateral pressures). Cases of wind-loaded shells were not treated as asymmetric loadings but some form of simplification was used to model axi-symmetric pressures.
- Terms "Reduced Stiffness" and "Reduced Energy" were used indistinctively in the literature. In some cases, although energy expressions were employed, reference to RSA was made.

This paper is concerned with extensions of the methodology to more complex engineering configurations in terms of loads and shell thicknesses, for which finite element analysis is mandatory in order to obtain results. Specifically, results are presented for cantilever cylindrical shells, both with and without a fixed roof.

2. Perturbation analysis

2.1. Classical bifurcation analysis

In its classical form, a stability analysis is limited to the solution of an eigenvalue problem, also known as LBA, and requires the computation of a linear equilibrium path as

$$\mathbf{K}^0\mathbf{a}^F + \lambda\mathbf{P} = \mathbf{0} \tag{2}$$

in which the linear stiffness matrix $\mathbf{K}^0$ of a shell has membrane and bending components, i.e. $\mathbf{K}^0 = \mathbf{K}^m + \mathbf{K}^b$.

Solution of the linear equilibrium problem at a load level (say $\lambda=1$) yields the displacements along the fundamental equilibrium path $\mathbf{a}^F$, from which the stress resultants $\mathbf{N}^F$ are obtained. This is an ingredient of the initial stress (or load-geometry) matrix $\mathbf{K}^G$ [29]

$$\mathbf{K}^G = -\int \boldsymbol{\beta}^T\mathbf{N}^F\boldsymbol{\beta}\,dA \tag{3}$$

where $\boldsymbol{\beta}$ is the rotation vector. In LBA, the following eigenvalue problem is solved:

$$\left[\left(\mathbf{K}^m + \mathbf{K}^b\right) - \lambda^C\mathbf{K}^G\right]\boldsymbol{\Phi}^C = \mathbf{K}^C\boldsymbol{\Phi}^C = \mathbf{0} \tag{4}$$

where the lowest eigenvalue λ^C is the classical critical load and $\boldsymbol{\Phi}^C$ is the associated eigenvector or critical mode, and $\mathbf{K}^C$ is a singular matrix at the critical state.

To understand the main concepts involved in the Reduced Energy/Stiffness Methods, it is instructive to consider first a perturbation expansion of the eigenvalue problem in LBA.

2.2. Perturbation via explicit substitution

Penalty parameters have been used in finite element analysis for some time (see for example Ref. [30], pp. 88). Consider the penalty parameter α as a scalar perturbation parameter, with values in the range $0<\alpha<1$, and we seek to obtain the solution to this problem in terms of α. The reason to introduce a penalty parameter in the formulation, rather than using a fixed value $\alpha=1$ to completely eliminate the membrane contribution is that the passage from the classical bifurcation analysis (LBA) to gradually decreasing the membrane contribution can be observed in more detail. This also serves to calibrate element performance through its evolution with α. The complete elimination of membrane action at the critical state is thus a limiting case which may introduce some computational difficulties.

If one assumes

$$\mathbf{K}^m(\alpha) = (1-\alpha)\mathbf{K}^m \tag{5}$$

Then the eigenvalue problem becomes

$$\left[(1-\alpha)\mathbf{K}^m + \mathbf{K}^b - \lambda^*\mathbf{K}^G\right]\Phi^* = \mathbf{0} \tag{6}$$

Notice that λ^* does not coincide with λ^C, and Φ^* is not the same as Φ^C. For $\alpha=0$, the classical eigenvalue problem is recovered, whereas for $\alpha=1$ the complete elimination of the membrane contribution is achieved. The exact solution of Eq. (6) is the basis of the RSA, in which the stiffness rather than the energy is affected by α. The solution can also be obtained by the perturbation analysis explored in this section up to quadratic perturbation terms.

The solution of this problem (in terms of the eigenvalue λ^* and eigenvector $\boldsymbol{\Phi}^*$) is expanded up to second order terms as

$$\begin{aligned}\lambda^*(\alpha) &= \lambda^{(0)} + \alpha\lambda^{(1)} + \frac{1}{2}\alpha^2\lambda^{(2)} + \cdots\\ \Phi^*(\alpha) &= \Phi^{(0)} + \alpha\Phi^{(1)} + \frac{1}{2}\alpha^2\Phi^{(2)} + \cdots\end{aligned} \tag{7}$$

Using the notation commonly employed in the General Theory of Elastic Stability [31,32], the unknowns in the expansion are derivatives with respect to the perturbation parameter as follows:

$$\lambda^{(n)} = \frac{d^n\lambda}{d\alpha^n}; \quad \Phi^{(n)} = \frac{d^n\Phi}{d\alpha^n} \tag{8}$$

The discussion that follows attempts to illustrate what contributions to Eq. (7) may be relevant in different cases. The term $\lambda^{(1)}$ is non-zero and it will be shown that there is a significant change in the eigenvalue due to the change in the stiffness as implied by α. But the contribution $\Phi^{(1)}$ depends on the specific load and shell configurations considered. Finally, the dependence of $\lambda^{(2)}$ on $\Phi^{(1)}$ will be shown, so that cases in which $\Phi^{(1)}=0$ do not present higher order contributions in λ.

At the critical state, the condition established in Eq. (4) is satisfied. To evaluate the unknowns and thus have the eigenvalue and eigenvector of the problem defined in Eq. (7) in explicit form, use is made of perturbation techniques. The variables in Eq. (7) are substituted into the original eigenvalue problem,

$$\begin{aligned}&\left[(1-\alpha)\mathbf{K}^m + \mathbf{K}^b - \left(\lambda^{(0)} + \alpha\lambda^{(1)} + \frac{1}{2}\alpha^2\lambda^{(2)}\right)\mathbf{K}^G\right]\\ &\quad\left(\Phi^{(0)} + \alpha\Phi^{(1)} + \frac{1}{2}\alpha^2\Phi^{(2)}\right)\\ &= 0\end{aligned} \tag{9}$$

The above equation is expanded and all terms with equal exponents in α are collected

$$\begin{aligned}&\alpha^0\left[\mathbf{K}^C\Phi^{(0)}\right]\\ &+\ \alpha^1\left[\mathbf{K}^C\Phi^{(1)} - \left(\mathbf{K}^m + \lambda^{(1)}\mathbf{K}^G\right)\Phi^{(0)}\right]\\ &+\frac{1}{2}\alpha^2\left[\mathbf{K}^C\Phi^{(2)} - 2\left(\mathbf{K}^m + \lambda^{(1)}\mathbf{K}^G\right)\Phi^{(1)} - \lambda^{(2)}\mathbf{K}^G\Phi^{(0)}\right]\\ &+\frac{1}{6}\alpha^3\left[\mathbf{K}^C\Phi^{(3)} - 3\left(\mathbf{K}^m + \lambda^{(1)}\mathbf{K}^G\right)\Phi^{(2)} - 3\lambda^{(2)}\mathbf{K}^G\Phi^{(1)}\right.\\ &\quad\left.+\cdots\right] + \cdots = 0\end{aligned} \tag{10}$$

According to the fundamental theorem of perturbations [33] because the perturbation parameter is independent of the expanded variables, Eq. (10) is zero only if each term multiplied by the perturbation parameter is independently zero. Thus, the perturbation equations of order zero, one, and two, become:

$$\begin{aligned}\mathbf{K}^C\Phi^{(0)} &= 0\\ \mathbf{K}^C\Phi^{(1)} &= \left(\mathbf{K}^m + \lambda^{(1)}\mathbf{K}^G\right)\Phi^{(0)}\\ \mathbf{K}^C\Phi^{(2)} &= 2\left(\mathbf{K}^m + \lambda^{(1)}\mathbf{K}^G\right)\Phi^{(1)} + \lambda^{(2)}\mathbf{K}^G\Phi^{(0)}\end{aligned} \tag{11}$$

The structure of all perturbation equations is similar. All lines contain the term $\mathbf{K}^C\boldsymbol{\Phi}^{(n)}$, but only for the zero-order perturbation equation this represents an eigenvalue problem, whereas for the higher order equations they are linear systems of equations. Further, the structure of terms on the right hand side is similar.

Because $\mathbf{K}^C$ is a singular matrix, the perturbation equations of order one and higher order contain fewer independent equations than unknowns, and to achieve a solution it is necessary to add another scalar condition. Solution of first order eigenvalue correction is achieved by use of the contraction mechanism [31], in which each term of the perturbation equation is pre-multiplied by the eigenvector $\boldsymbol{\Phi}^{(0)}$, and because of symmetry of the system, the term on the left of Eq. (11) becomes zero. This allows computing the derivatives of the load factor before computing the derivatives of the critical mode. Using this procedure, the first and second order contracted forms become:

$$\Phi^{(0)T}\left(\mathbf{K}^{m}+\lambda^{(1)}\mathbf{K}^{G}\right)\Phi^{(0)}=0$$
$$2\Phi^{(0)T}\left(\mathbf{K}^{m}+\lambda^{(1)}\mathbf{K}^{G}\right)\Phi^{(1)}+\lambda^{(2)}\Phi^{(0)T}\mathbf{K}^{G}\Phi^{(0)}=0 \quad (12)$$

Notice that the contracted form of the perturbation equations are values of energy, as employed in the REA.

2.3. First order perturbation terms

In Eq. (10), terms that multiply α^0 are the zero-order perturbation equation, which is a classical eigenvalue problem and can be solved to obtain the scalar $\lambda^{(0)}$ and the vector $\mathbf{\Phi}^{(0)}$. Also in Eq. (10), the terms multiplied by α^1 form the first-order perturbation equation and are the second line in Eq. (11). In this case, there are more independent unknowns than conditions, so that use of the contraction mechanism is required. The contracted form of this equation is the first line in Eq. (12), from which

$$\lambda^{(1)}=-\frac{\Phi^{(0)T}\mathbf{K}^{m}\Phi^{(0)}}{\Phi^{(0)T}\mathbf{K}^{G}\Phi^{(0)}} \quad (13)$$

Clearly, $\lambda^{(1)}$ is not zero and there is at least a first-order effect on the eigenvalue. Notice that from the zero-order perturbation equation, one can write

$$\Phi^{(0)T}\mathbf{K}^{G}\Phi^{(0)}=\frac{1}{\lambda^{(0)}}\Phi^{(0)T}\left(\mathbf{K}^{m}+\mathbf{K}^{b}\right)\Phi^{(0)} \quad (14)$$

Thus, substituting Eq. (14) into (13) yields

$$\lambda^{(1)}=-\frac{\Phi^{(0)T}\mathbf{K}^{m}\Phi^{(0)}}{\Phi^{(0)T}\left(\mathbf{K}^{m}+\mathbf{K}^{b}\right)\Phi^{(0)}}\lambda^{(0)} \quad (15)$$

All terms in the above equation can be computed using ABAQUS [34], ANSYS [35] or other general purpose finite element programs. The negative value of $\lambda^{(1)}$ is consistent with the reduction assumed in $\mathbf{K}^{m}$. This scalar can be computed from Eq. (15) using the available results.

To continue with the evaluation of the eigenvector derivative $\varphi^{(1)}$, we now return to the first order perturbation equation (second line in Eq. (11))

$$\mathbf{K}^{C}\Phi^{(1)}=\left(\mathbf{K}^{m}+\lambda^{(1)}\mathbf{K}^{G}\right)\Phi^{(0)} \quad (16)$$

$\mathbf{K}^{C}$ is a singular matrix, which brings some additional difficulties into the solution.

There are two ways to obtain the first order derivative $\varphi^{(1)}$: the first one is to solve it directly from the Eq. (16). Because the buckling mode which participates in the eigen-problem does not have a specific norm, what is usually done is to assign a unit value to one of the components and calculate the rest using this scaling rule. Without loss of generality, we can assume that the largest component in φ is the first one, and normalize it in the form $\varphi_1=1$. This yields ${\varphi_1}^{(0)}=1$, and null values for the derivatives of the first component, ${\varphi_1}^{(1)}={\varphi_1}^{(2)}=0$. Under these conditions, Eq. (16) can be solved. In practical terms, this can be performed by elimination of the first column in Eq. (16) (because ${\varphi_1}^{(1)}=0$) and the first row to keep the symmetry in the system.

There is an alternative way to solve $\Phi^{(1)}$, which is to impose the condition that the derivatives of the buckling mode should be orthogonal to the original eigenvector.

This completes the computation of variables in the first order perturbation equation.

The value of first derivative of λ, i.e. $\lambda^{(1)}$, is non-zero, so that there is an effect of α on the eigenvalue. However, not necessarily there is an effect on the eigenvector: This is a very common situation, and we shall find examples of this in the forthcoming sections.

2.4. Second order perturbation terms

To obtain the second order derivatives one must return to the second order perturbation equation (third line in Eq. (11)). The contracted form of the second order perturbation equation (second line in Eq. (12)) becomes

$$2\ \Phi^{(0)T}\left(\mathbf{K}^{m}+\lambda^{(1)}\mathbf{K}^{G}\right)\Phi^{(1)}+\lambda^{(2)}\Phi^{(0)T}\mathbf{K}^{G}\Phi^{(0)}=0 \quad (17)$$

where the unknown $\lambda^{(2)}$ can be solved as

$$\lambda^{(2)}=-2\frac{\Phi^{(0)T}\left(\mathbf{K}^{m}+\lambda^{(1)}\mathbf{K}^{G}\right)\Phi^{(1)}}{\Phi^{(0)T}\mathbf{K}^{G}\Phi^{(0)}} \quad (18)$$

or else, in terms of the stiffness matrix K^0,

$$\lambda^{(2)}=-2\ \frac{\Phi^{(1)T}\left(\lambda^{(0)}\mathbf{K}^{m}+\lambda^{(1)}\mathbf{K}^{0}\right)\Phi^{(0)}}{\Phi^{(0)T}\mathbf{K}^{0}\Phi^{(0)}} \quad (19)$$

Notice that if $\Phi^{(1)}$ was zero, then $\lambda^{(2)}$ would also be zero, and the problem would only have first-order changes.

The second derivative of the eigenmode can be computed from the second order perturbation equation, third line in Eq. (11)

$$\mathbf{K}^{C}\Phi^{(2)}=2\left(\mathbf{K}^{m}+\lambda^{(1)}\mathbf{K}^{G}\right)\Phi^{(1)}+\lambda^{(2)}\mathbf{K}^{G}\Phi^{(0)}$$

in a way similar to the first order. Under the assumed normalization, the first component ${\Phi_1}^{(2)}$ should be zero, and this can be implemented by deleting the first column and the first row.

The perturbation analysis presented above is not currently an alternative way to carry out the computations, but it is mainly a way to help explaining what is retained and what is missing in RSA and REA. However, it cannot be easily solved using a general purpose code, except for $\lambda^{(1)}$.

The above ideas will be next employed as a background to discuss lower bound using RSA and REA strategies.

3. Reduced Stiffness Analysis (RSA)

The procedures for implementation of the Reduced Stiffness Analysis (RSA) and Reduced Energy Analysis (REA) and have been reviewed in [27] and [37], just to cite a couple of references. The necessary background to the energy approach to investigate stability of elastic systems was originally developed by Koiter for continuous systems [2], followed by developments for discrete systems [31,32].

3.1. Methodology

The RSA (also the REA presented in the next section) starts by exploring the energy components of the shell in the classical eigenmodes, including membrane and bending energy contributions and load potential. Depending on the shell and load considered, some of these energy contributions are positive and others are negative. Positive energy components contribute to the stability of the shell, whereas negative components tend to de-stabilize the shell. The main assumption in the RSA is that positive stabilizing components are lost in the buckling process due to coupling between geometric imperfections and nonlinear effects. Under lateral pressure, it has been shown that membrane components are eroded in cylindrical shells [27]. Thus, reducing the membrane energy contribution is carried out in the RSA, and in the limit, as the membrane contribution is eliminated, a lower bound is reached. This approach has been extensively validated for simple shells by comparison with experiments and with GNIA computations, at least for cases of uniform pressure.

In the RSA membrane components in the linear stiffness matrix $\mathbf{K}$ are selectively eliminated, but this may be more conveniently written in terms of a penalty approach using a penalty parameter α, as explained in the previous section, with values between zero and one. The modified LBA becomes Eq. (6),

$$\left[\left((1-\alpha)\,\mathbf{K}^{\mathrm{m}}+\mathbf{K}^{\mathrm{b}}\right)-\lambda^{*}\mathbf{K}^{\mathrm{G}}\right]\boldsymbol{\Phi}^{*}=0$$

The solution of this modified eigenvalue problem is identified as λ^*, $\boldsymbol{\Phi}^*$, which depend on the adopted value of α. If $\alpha\to 1$, then the formulation becomes the classical RSA. It has been shown that a lower bound is obtained for α close to one, and not necessarily one [38,39].

Notice that the equilibrium condition yielding $\mathbf{N}^{\mathrm{F}}$ is not affected by α. The linear equilibrium path that serves to identify λ^{C} is the same path from which λ^* is calculated.

The knock-down factor η is usually employed to normalize results in the form

$$\lambda^{*}=\eta\lambda^{\mathrm{C}} \tag{20}$$

Because $\boldsymbol{\Phi}^*$ has not been limited to coincide with $\boldsymbol{\Phi}^{\mathrm{C}}$, the eigenmodes may change from the classical analysis to the RSA, thus providing more flexibility to the analysis. Thus, higher order terms in the perturbation expansion described in Eq. (7) are automatically taken into account.

The drawback of RSA is that the procedure can only be implemented in a special purpose code by modification of the formulation [40,41], but it has not yet been possible to implement it in general purpose code like ABAQUS or ANSYS.

3.2. Additional complexities faced in practical engineering situations

In many shell problems, the structural analysis requires taking into account the step-wise variable thickness of the cylindrical shell. In fluid storage tanks, this is a consequence of having variable pressures in height, and the technological constraint to fabricate the shell by means of courses each with uniform thickness. This induces buckling modes that affect the top (thinner) courses of the cylinder, whereas no significant displacements occur in the lower (thicker) courses.

A second important feature arises under wind pressures: buckling is dominated by positive pressures at windward and the buckling mode is localized in that region, so that small displacements occur around the circumference away from windward.

Those differences in regions for which large displacements are expected at buckling versus regions unaffected by a buckling mode poses new questions not envisaged under uniform pressure/uniform thickness configurations: On what part of the shell is the membrane contribution being eroded at buckling as a consequence of imperfection sensitivity? Should this stiffness erosion be assumed on the complete surface of the shell (here identified as Complete RSA) or should it be restricted to the region in which the LBA buckling mode occurs? In the last case (which is here identified as Selective RSA), how do large stepwise changes in membrane stiffness between regions with reduced membrane contribution affect the evaluation of modes consistent with GNIA? Some of these questions are next discussed with reference to examples.

4. Reduced Energy Analysis (REA)

The Reduced Energy Analysis (REA) has been described by Croll and co-workers [27,28], and a slightly different formulation was given in Ref. [37]. An alternative brief presentation is given next, in which it is shown that the method can be derived from the perturbation equations of Section 2.

4.1. Methodology

Returning to the expansion of the eigenvalue defined in the first line of Eq. (7), up to first order terms, the solution reads

$$\lambda=\lambda^{(0)}\left(1-\alpha\frac{\boldsymbol{\Phi}^{(0)\mathrm{T}}\mathbf{K}^{\mathrm{m}}\boldsymbol{\Phi}^{(0)}}{\boldsymbol{\Phi}^{(0)\mathrm{T}}\left(\mathbf{K}^{\mathrm{m}}+\mathbf{K}^{\mathrm{b}}\right)\boldsymbol{\Phi}^{(0)}}\right) \tag{21}$$

After some algebraic manipulation, this can be written in the form

$$\lambda=[1-\alpha(1-\eta)]\lambda^{(0)} \tag{22}$$

where

$$\eta=\frac{\boldsymbol{\Phi}^{(0)\mathrm{T}}\mathbf{K}^{\mathrm{b}}\boldsymbol{\Phi}^{(0)}}{\boldsymbol{\Phi}^{(0)\mathrm{T}}\left(\mathbf{K}^{\mathrm{m}}+\mathbf{K}^{\mathrm{b}}\right)\boldsymbol{\Phi}^{(0)}} \tag{23}$$

This value of η has been identified as the knock-down factor in the REA [27]. Eqs. (22) and (23) are the basis of the REA, in which the energy is reduced by a factor α. Because the classical eigenvector $\boldsymbol{\Phi}^{(0)}$ has been used up to this point, then the modified eigenvalue has been calculated based on the unmodified eigenvector.

The extreme value $\alpha=1$, for which complete annihilation of the membrane contribution occurs, leads to

$$\lambda^{*}=\eta\lambda^{(0)}\ \text{ else }\ \eta=\frac{\lambda^{*}}{\lambda^{(0)}} \tag{24}$$

which is the lower bound λ^* employed in Croll's work [27].

In the Theory of Elastic Stability, the following notation is usually employed [32]

$$\mathrm{U}^{2\mathrm{m}}=\boldsymbol{\Phi}^{(0)\mathrm{T}}\mathbf{K}^{\mathrm{m}}\boldsymbol{\Phi}^{(0)}\quad\text{and}\quad\mathrm{U}^{2\mathrm{b}}=\boldsymbol{\Phi}^{(0)\mathrm{T}}\mathbf{K}^{\mathrm{b}}\boldsymbol{\Phi}^{(0)} \tag{25}$$

in which $\mathrm{U}^{2\mathrm{m}}$ and $\mathrm{U}^{2\mathrm{b}}$ are energy components in the critical mode. Substituting into Eq. (25), one can write

$$\eta=\frac{\mathrm{U}^{2\mathrm{b}}}{\mathrm{U}^{2\mathrm{m}}+\mathrm{U}^{2\mathrm{b}}} \tag{26}$$

This is the knock-down factor used in the REA if the membrane energy is completely eliminated, and the results coincide with those of Eq. (1).

One of the limitations of implementing this REA in a general purpose code like ABAQUS is that it does not allow for separate computation of membrane and bending energy components, which are merged in any finite element package.

4.2. Metal shells modeled as a composite material

Sosa et al. [37] showed a simple way to implement the REA by modeling the isotropic metal shell as a composite material. Thus, by assuming a more complex material model, one may employ a constitutive matrix of a composite as in Classical Lamination Theory [42] [43]

$$\begin{Bmatrix}\mathbf{N}\\ \mathbf{M}\end{Bmatrix}=\begin{bmatrix}\mathbf{A} & \mathbf{B}\\ \mathbf{B}^{\mathrm{T}} & \mathbf{D}\end{bmatrix}\begin{Bmatrix}\varepsilon\\ \kappa\end{Bmatrix} \tag{27}$$

where $\mathbf{A}$ is the membrane sub-matrix, whereas the bending sub-matrix is $\mathbf{D}$, given as

$$\mathbf{A}=\begin{bmatrix}\mathrm{A}_{11} & \mathrm{A}_{12} & 0\\ \mathrm{A}_{21} & \mathrm{A}_{22} & 0\\ 0 & 0 & \mathrm{A}_{33}\end{bmatrix}\quad\mathbf{D}=\begin{bmatrix}\mathrm{D}_{11} & \mathrm{D}_{12} & 0\\ \mathrm{D}_{21} & \mathrm{D}_{22} & 0\\ 0 & 0 & \mathrm{D}_{33}\end{bmatrix} \tag{28}$$

where **B** is the bending-extension coupling matrix, which is a null matrix for symmetric laminates. The REA is implemented by adopting a reduction in all or selected membrane components of **A** with a penalty parameter α. Notice that by affecting the membrane energy of the shell, a different shell theory is being assumed.

The REA computations follow this sequence:

- The classical eigenvalue problem is solved, leading to λ^C, $\mathbf{\Phi}^C$.
- The mode shape $\mathbf{\Phi}^C$ is imposed as a displacement field in a linear static analysis of the shell as a composite with $\alpha=1$. The strain energy is computed, and this is the term $(U^{2m}+U^{2b})$.
- The mode shape $\mathbf{\Phi}^C$ is imposed as a displacement field in a linear static analysis of the shell as a composite with $\alpha\neq1$. The strain energy is computed. This is $[(1-\alpha)\,U^{2m} + U^{2b}]$.
- The reduced load is calculated as the ratio between reduced and full energy values at the critical state.

5. Numerical results for cylindrical shells with a fixed conical roof

Benchmarks for vertical aboveground tanks have been developed by the authors in previous works and are employed here to highlight features and shortcomings of the methodology under discussion. These benchmarks have been extensively used in the literature to investigate buckling of fluid storage tanks.

5.1. Geometry of the shells considered

A set of six tanks with conical roof having $0.24 < H/D < 0.95$ and variable thickness was originally investigated by Virella et al. [44] as a benchmark. Interest in these cases arises because the buckling modes are localized at the top courses of the cylinder and the static buckling behavior and imperfection sensitivity are almost the same. Essentially, this is a problem dominated by bifurcation behavior and as such the benchmark is representative of a class of shell problems.

The specific geometries considered are shown in Fig. 1, where each model is identified as MC1–MC6. In all cases reported in this paper, American Petroleum Institute [45] regulations were used to evaluate the shell thickness (Table 1).

5.2. Shells under uniform pressure, for which the LBA eigenvector is a good approximation (or $\Phi^{(1)}=0$)

5.2.1. LBA and GNIA results under uniform pressure

For each configuration of this benchmark, LBA computations were performed under uniform pressure using ABAQUS to find the classical critical load λ^C; and some results are indicated in Fig. 2 for MC2, MC4, and MC6. The buckling modes have a sinusoidal shape with a number of circumferential waves j that depend on the H/D configuration. For example, the eigenvector for MC2 has 23 full waves in the circumferential direction.

Table 1
Tanks with conical roof. Thickness at each steel course for models MC1 to MC6.

Shell course	MC1 t [mm]	MC2 t [mm]	MC3 t [mm]	MC4 t [mm]	MC5 t [mm]	MC6 t [mm]
1	9.5	12.7	17.5	20.6	25.4	28.6
2	7.9	11.1	15.9	17.5	22.2	25.4
3	7.9	7.9	12.7	15.9	20.6	25.4
4		7.9	11.1	12.7	17.5	22.2
5		7.9	9.5	11.1	15.9	20.6
6			7.9	7.9	12.7	19.1
7			7.9	7.9	11.1	15.9
8				7.9	7.9	12.7
9					7.9	11.1
10					7.9	7.9
11						7.9
12						7.9

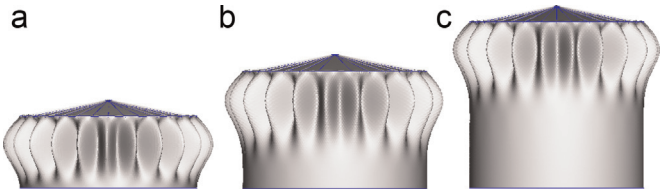

Fig. 2. Tanks with conical roof, LBA buckling modes for (a) Tank MC2: $\lambda^C=2.159$, $j=23$; (b) Tank MC4: $\lambda^C=2.323$, $j=21$; and (c) Tank MC6: $\lambda^C=2.314$, $j=21$.

GNIA was also performed for the shells using eigenvector-affine imperfections, i.e. imperfections with the same shape as the LBA eigenvector associated with λ^C. Computational evaluation of the nonlinear equilibrium path is a relatively simple task using commercial software like ABAQUS or ANSYS. Results of equilibrium paths are shown in Fig. 3 for four of the tanks (MC1, MC2, MC4, MC6) and for different imperfection amplitudes expressed as fractions of the minimum course thickness (t_{min}) corresponding to each model.

The knock-down factor η depends on ξ and reduces from $\eta=1$ at $\xi=0$ (perfect shell) to a value given by the maximum in the path.

In MC1, $\xi/t_{min}=0.5$ is the imperfection amplitude for which a maximum still exists in the equilibrium path and η becomes 0.72 for that case. For higher amplitudes ξ the path does not show a maximum and the problem ceases to be dominated by buckling. All six cases have similar imperfection-sensitivity curves as illustrated in Fig. 4, with $\eta=0.72$.

Finally, the mode shape at buckling as computed from LBA is the same as the mode identified via GNIA at the maximum in the equilibrium path; this is an important result because it indicates that one should not expect to have a mode change in the RSA or the REA. In terms of the perturbation expansion presented in Section 3, this means that the first-order eigenvector correction is zero, i.e. $\mathbf{\Phi}^{(1)}=\mathbf{0}$.

An analysis of the energy contributions at the critical state (as obtained from LBA) for different harmonics is shown in Fig. 5 for MC4. Unlike the case of a cantilever cylinder, the shell with a fixed

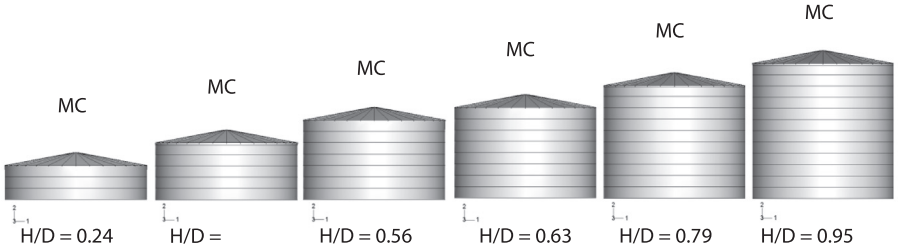

Fig. 1. Tanks with conical roof, MC1–MC6, with step-wise variable thickness.

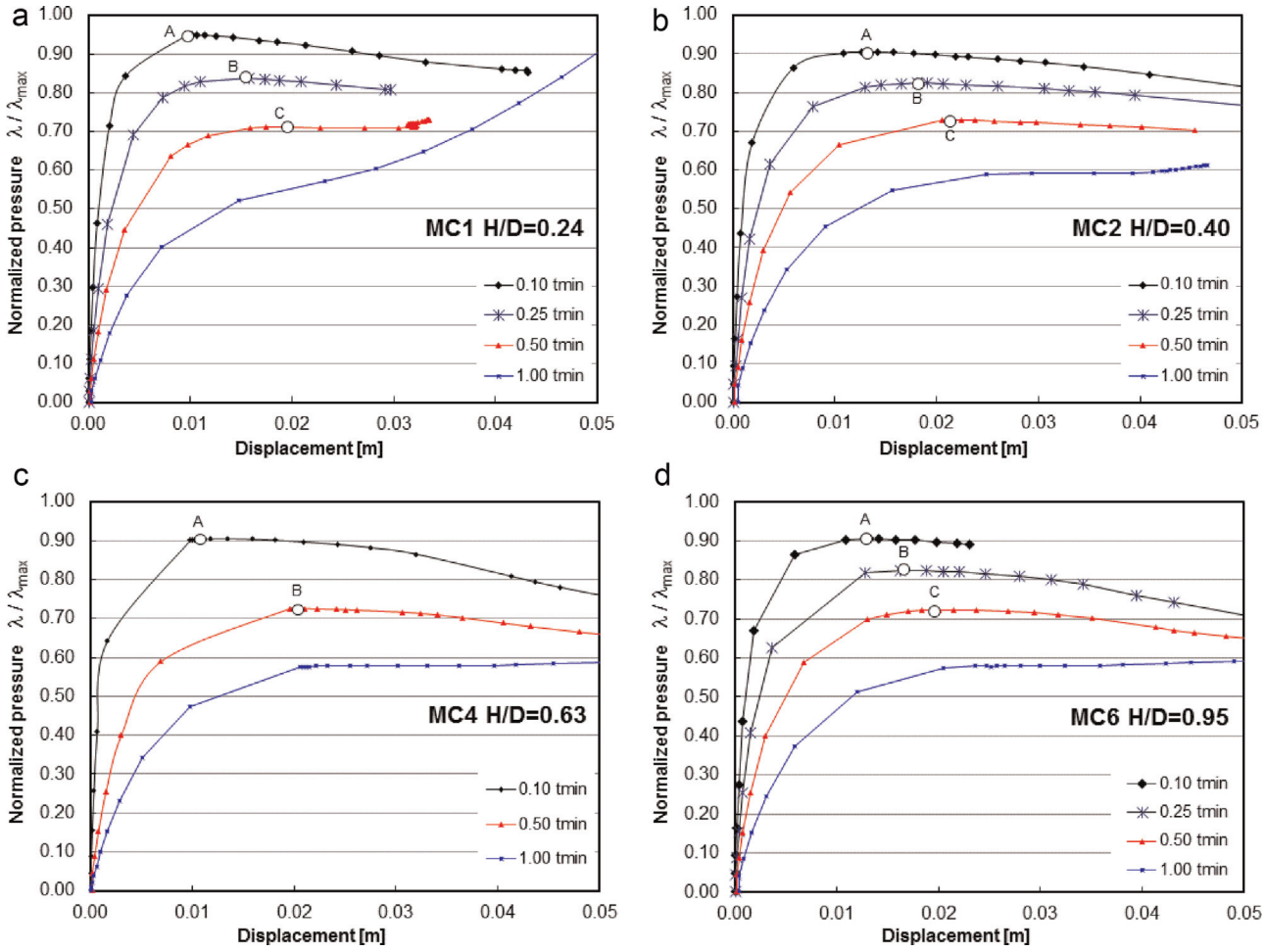

Fig. 3. Cylindrical shells with conical roof under uniform pressure, GNIA results. Equilibrium paths for different imperfection amplitudes. (a) Model MC1, $H/D=0.24$; (b) Model MC2, $H/D=0.40$; (c) Model MC4, $H/D=0.63$; and (d) Model MC6, $H/D=0.95$.

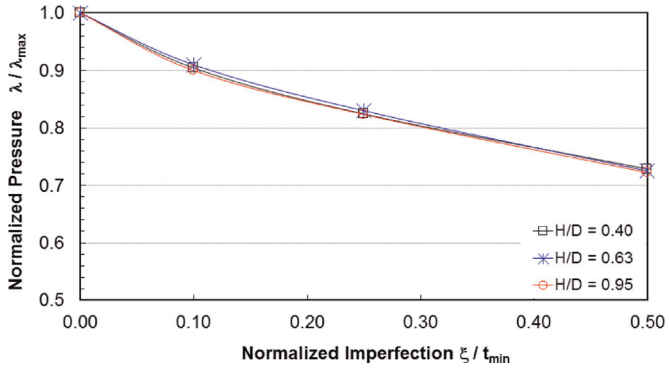

Fig. 4. Compilation of imperfection sensitivity curves for models MC2, MC4, MC6 under uniform pressure.

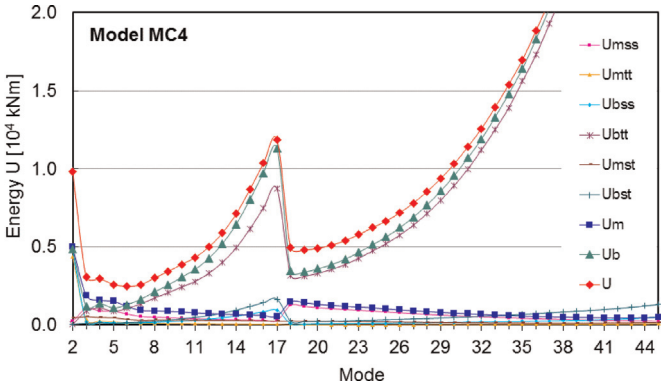

Fig. 5. Tanks with conical roof, energy contributions for model MC4, as a function of number of circumferential waves j.

roof does not show a unique minimum but has two: one is associated with the cylinder and the second one is due to the influence of the roof.

For a low number of circumferential waves $j=5$ there is a minimum due to the cylinder mode, whereas a second local minimum occurs for $j=18$. Regarding energy components, the membrane contribution dominates low j modes, which rapidly decays with an increase in bending contribution. But there is a new increase in membrane component prior to the second local minimum and a decrease in bending contribution. Passing the second minimum, the membrane energy decays and the bending energy increases.

For the first local minimum, 82% of U^m is contributed by the meridional component U^m_{ss} and 17% is due to the shear U^m_{st}. The hoop contribution U^m_{tt} is negligible in this case.

5.2.2. *Application of RSA*

A lesson learned from the perturbation analysis is that one should consider the possibility of having changes in both eigenvalue and eigenvector. However, there are situations in which $\mathbf{\Phi}^{(1)}=0$, so that $\mathbf{\Phi}^{(0)}=\mathbf{\Phi}^C$ is the critical mode. This can be observed by comparison of between the classical LBA and the GNIA modes.

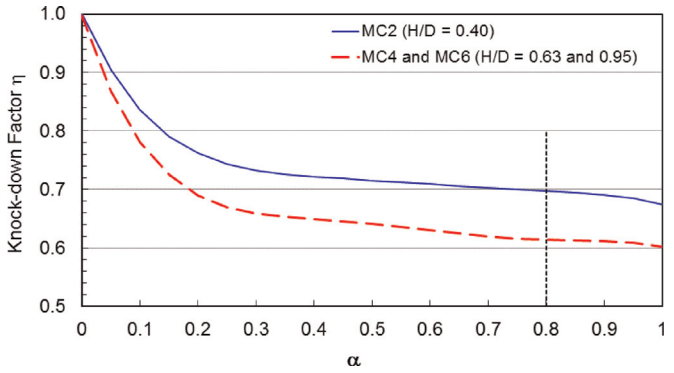

Fig. 6. Tanks with conical roof, under uniform pressure. RSA results for Tanks MC2, MC4, and MC6.

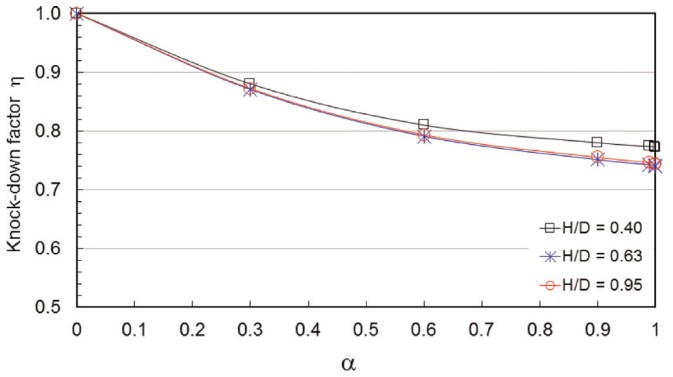

Fig. 7. Tanks with conical roof, uniform pressure. REA results for Tanks MC2, MC4, and MC6.

Implementation of the RSA has been carried out in this case using a special purpose semi-analytical finite element code ALREF [40], which is capable of performing LBA as well as initial post-critical behavior [36,41]. Because this is an in-house code, changes in the computations can be easily introduced to reduce the membrane contribution to the stiffness of the shell.

Plots of η versus penalty parameter α are shown in Fig. 6 for stiffness reductions affecting the cylinder, whereas the stiffness of the roof remains unchanged. Each curve shows a decrease in η with increasing α, but this change is severe for $0<\alpha<0.4$ and far less pronounced for higher values of α.

Shell configuration MC2 ($H/D=0.4$) shows for $\alpha=1$ in Fig. 6 a lower bound equal to $\eta=0.67$, which is 7% lower than the value obtained with GNIA. The results for MC4 and MC6 for $\alpha=1$ tend to $\eta=0.6$, which is 17% lower than that given by GNIA. Thus, the knock-down factors calculated with RSA with $\alpha=1$ represent a lower bound with respect to nonlinear analysis and can be used with confidence.

In this research we are also interested in the identification of the buckling mode, so that results with RSA were obtained in all cases and for all values of α. It was found that the quality of the mode becomes poor as α approaches 1, because the complete elimination of membrane energy produces excessive flexibility. The problem can be solved if $\alpha=0.9$ is adopted for the mode in all cases instead of $\alpha=1$. Notice that knock-down factors slightly increase for $\alpha=0.9$, being 4% lower than GNIA for $H/D=0.4$, and 12.5% lower than GNIA for $0.63<H/D<0.95$.

5.2.3. Application of REA

The equivalent composite material has been employed to solve the same benchmark. Eight different finite elements implemented in ABAQUS were initially investigated to perform computations, and it was found that element STRI3, a fully integrated triangular element originally developed by Batoz et al. [46], showed the best performance by converging to the analytical solution of REA [37].

The lower bounds results obtained with GNIA (Fig. 4) show that the mode shape does not a change between the classical LBA and the GNIA computations.

Fig. 7 shows the REA by means of the penalty approach for MC1, MC2, MC4, and MC6. Imperfection sensitivity in cases MC2, MC4, and MC6 should be approximately the same because the tanks buckle at the top of the cylinder in a local mode.

Under uniform pressure, the results are close to $\eta=0.72$ obtained with GNIA. One of the differences shown in Fig. 7 is that not all three cases considered tend to the same value as the penalty parameter α tends to 1: the shorter tank (MC2, $H/D=0.40$) tends to $\eta=0.77$, a slightly higher value than $\eta=0.74$ obtained for the other two cases (MC4 and MC6, i.e. $H/D=0.63$ and 0.95). Although these results do not represent a true lower bound to GNIA, they are sufficiently close (7% and 3% higher) as to be used with confidence.

Unlike what was observed in RSA, the present results using REA tend to a constant value as $\alpha\to 1$. Notice that there is a remarkable similarity between the curves of knock-down factor η in terms of perturbation parameter in Fig. 7 and those of imperfection-sensitivity in Fig. 4.

Modes are not calculated using REA since the eigenvector associated with the lowest classical eigenvalue in LBA is assumed to occur at the lower bound.

REA results under uniform pressure are encouraging and show a possible way to implement the methodology in finite element software like ABAQUS, without introducing any modification in the code, simply by using its present capabilities.

5.3. Shells under wind pressure, for which the LBA eigenvector is not a good approximation (or $\Phi^{(1)}\neq 0$)

Wind buckling of thin-walled shells has been extensively illustrated in the literature for individual shells, as well as overall reports of buckling of many tanks occurred during one wind storm [47]. Shell problems under wind loading are typical cases in which the classical bifurcation eigenmode does not coincide with that obtained from GNIA. The only early work involving wind pressures were reported by Zintillis and Croll [14] for hyperboloids of revolution (cooling tower shells); however, buckling using REA was estimated for axisymmetric pressure and the results were extended to wind by adopting the "Worst Stress Meridian" and "Worst Pressure Meridian" methods. Comparisons with wind tunnel tests showed differences in the order of 30%, and a number of reasons may serve to explain such differences.

5.3.1. LBA and GNIA studies under wind pressure

Wind pressures were modeled according to ASCE 7 [3]. Under wind pressure, the buckling mode computed by LBA is localized in the region at windward and on the top courses of the shell, where the thickness is a minimum, as shown in Fig. 8. It can be seen from the plots that the buckling region is almost identical in all cases except for MC1, in which case the shell is so short that it cannot develop the same mode as in the other cases. The lowest eigenvalue ($\lambda^C=2.50$ KPa) is computed for the tallest shell MC6, with $H/D=0.95$ (Table 2).

GNIA studies for the same shells under wind were computed with ABAQUS, and plots for MC1, MC2, MC4 and MC6 are shown in Fig. 9. For imperfections up to $\xi=1.0\ t_{\min}$, the equilibrium paths show a maximum before the path drops.

The imperfection-sensitivity curve (Fig. 10) indicates a knock-down factor of $\eta=0.66$ for $H/$ $=0.24$, and $\eta=0.58$ for the other three cases; these are lower values than those obtained under

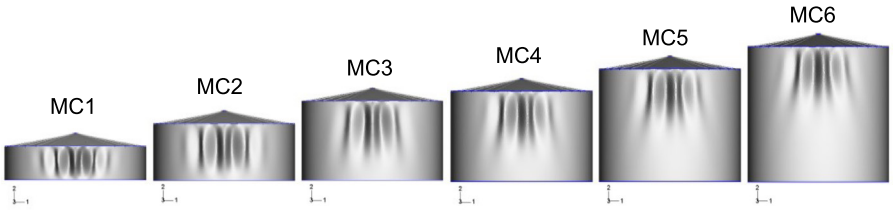

Fig. 8. Tanks with conical roof, under wind pressure. Lowest eigenvectors λ^C obtained by LBA.

Table 2
Tanks with conical roof, under wind pressure. Lowest eigenvalue obtained with LBA (ALREF).

Model	MC1	MC2	MC3	MC4	MC5	MC6
H/D	0.24	0.40	0.56	0.63	0.79	0.95
λ^C [KPa]	3.89	2.55	2.92	2.51	2.54	2.50

uniform pressure, and are target values which should be estimated by lower bound methods as RSA and REA.

Some of the key differences between wind loaded and uniform pressure loaded shells are first, mode localization, and second, mode differences between LBA and GNIA.

5.3.2. *Application of RSA: complete reduction in membrane contribution*

The in-house code ALREF [40] was used to perform the RSA computations, with changes in the code to account for reductions in the membrane contribution. Implementation of RSA in this case involves reducing U_{ss}^m and $U_{ss}^m + U_{st}^m$ by using a penalty parameter α.

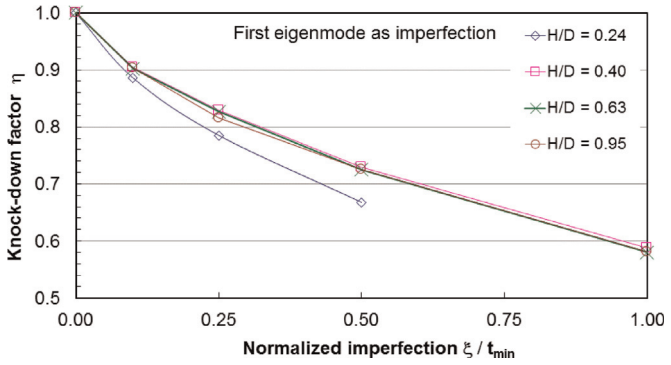

Fig. 10. Imperfection-sensitivity using eigenvector-affine imperfection.

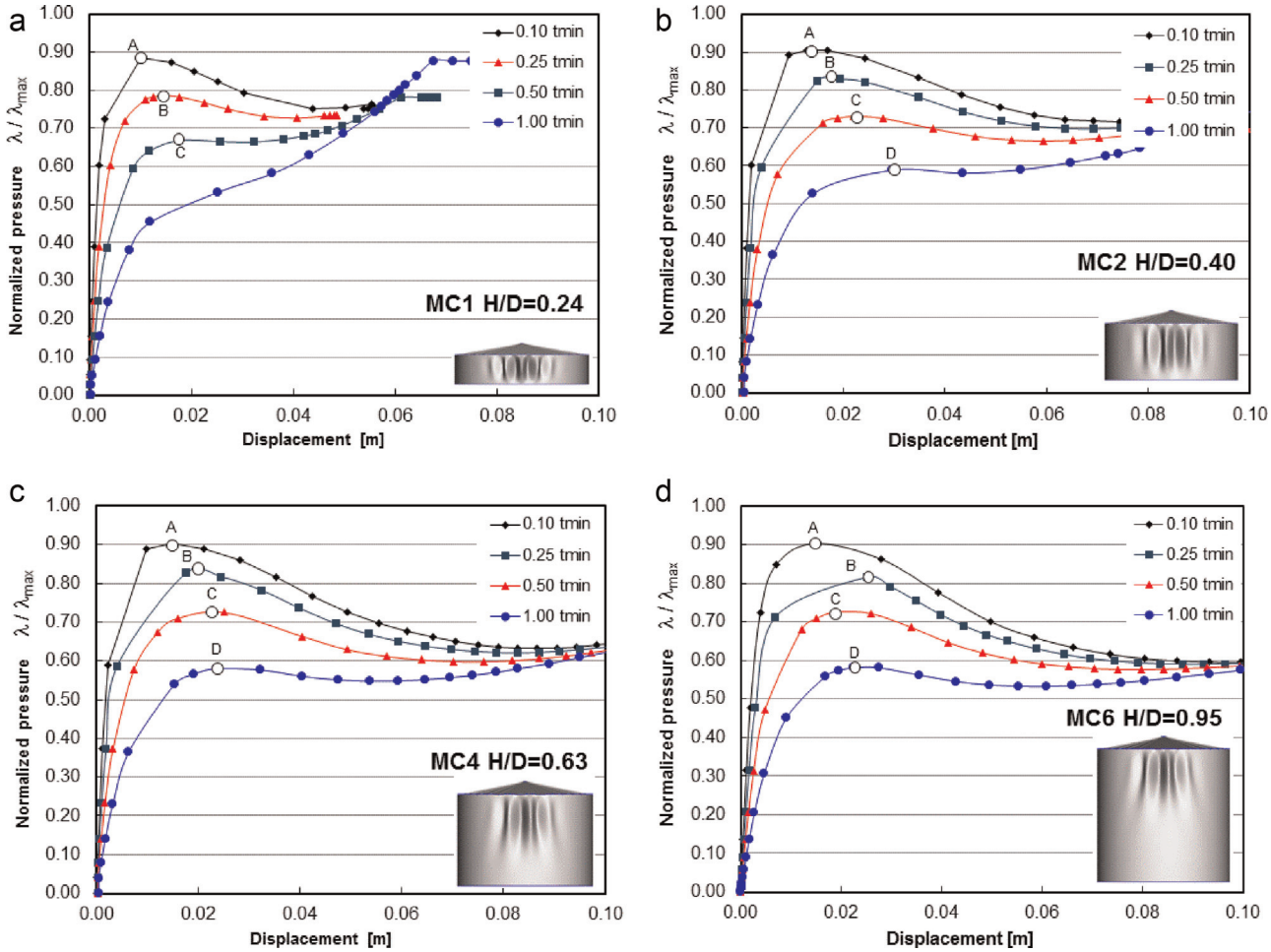

Fig. 9. GNIA results under wind pressures, nonlinear equilibrium paths for different imperfection amplitudes. (a) Model MC1, $H/D=0.24$; (b) Model MC2, $H/D=0.40$; (c) Model MC4, $H/D=0.63$; and (d) Model MC6, $H/D=0.95$.

As a first approach, the RSA was applied to the complete cylindrical shell, so that reductions in membrane stiffness were adopted on the complete cylindrical shell. This is a questionable approach, since there are regions of the shell which are not affected by the buckling mode, and their stiffness would anyway be reduced, thus modeling a very flexible shell. Results for $\alpha=1$ are summarized in Table 3, and show reductions more severe than those obtained with GNIA.

In this case, there are differences in mode shape between LBA and GNIA solutions. Correct buckling modes predicted by GNIA present large deflections only in the windward region, with an effect known as "mode attenuation" around the circumference, thus becoming a localized mode. For the leeward region of the shell there are small deflections as obtained from classical buckling studies. The mode localization affects not just the meridional but also the circumferential direction.

5.3.3. Application of RSA: selective reduction in membrane contribution

An improved solution is obtained by using a selective stiffness reduction, in which only the regions in which a buckling mode develops are affected by a reduction. This region affects the top courses (with thinner shell, where buckling occurs). Numerical results are shown in the last column of Table 3 for $\alpha=1$, and in Fig. 11 for all values of α. Differences in η with respect to GNIA are of 23% for $H/D=0.24$, 12% for $H/D=0.40$, and 3% for $0.63<H/D<0.95$.

The results in a plot η versus α in Fig. 11 are lower than GNIA as $\alpha\to 1$, but the complete elimination of membrane stiffness ($\alpha=1$) contribution around the circumference under wind yields a spurious mode. To get the correct eigenmode, some membrane energy must be retained in the analysis, and this can be done by adopting a value of α in the order of 0.80 instead of 1.

Thus, improving the solution in this case requires that the method should be applied on the part of the shell in which a buckling mode develops. Using semi-analytical finite element codes like ALREF [40] or BOSOR [49], this can be done in the vertical direction to account for thickness variations, but establishing zones around the circumference with variations in membrane stiffness is not possible. Assigning different stiffnesses in the circumferential direction requires the use of fully two-dimensional shell elements. A more detailed discussion of implementing RSA in cases under wind may be found in [50].

5.3.4. Application of REA

Wind loaded shells display such behavior that one cannot assume that the classical eigenmode is also the same deflection pattern associated with GNIA or the penalty formulation.

As said before, the lower bound using GNIA is $\eta=0.6$. REA, on the other hand, provided higher values in the range $\eta=0.76$–0.79, and with small variations among them, as seen in Fig. 12. This convergence of REA to higher knock-down factors than GNIA remains as a challenge to the REA, and, as reported by [48], the problem has not been solved at present.

Table 3
Tanks with conical roof, under wind pressure. Results of RSA for wind loaded shells MC1–MC6, with penalty parameter $\alpha=1$.

Case	H/D	η	
		U^m–U^m_{ss}–U^m_{st} (reduction in the complete cylinder)	U^m–U^m_{ss}–U^m_{st} (reduction in the top courses)
MC1	0.24	0.51	–
MC2	0.40	0.51	0.51
MC4	0.63	0.54	0.56
MC6	0.95	0.56	0.56

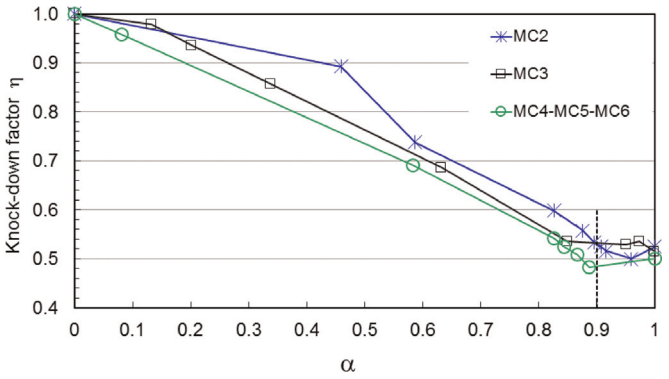

Fig. 11. Tanks with conical roof, wind pressure. RSA results using selective stiffness reduction.

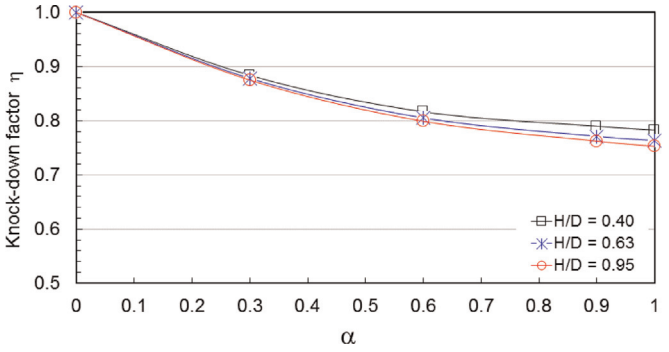

Fig. 12. Tanks with conical roof, wind pressure. REA. As reference, the lower bound using GNIA is $\eta=0.6$.

6. Numerical results for cantilever cylindrical shells

The simplest form of storage tank is a cantilever cylinder which is opened at the top. However, this shell form behaves in a very different way from shells with a roof, and their buckling modes under wind occur in a limit point type of behavior. Because of space constraints, only problems under wind will be discussed in this section.

6.1. Geometry of the shells considered

To illustrate the use of RSA and REA methodologies, cantilever cylindrical shells with differences in geometric characteristics are considered, as shown in Fig. 13. The benchmark was originally discussed by Godoy and Flores [51]. In Fig. 13 and Table 4, the Batdorf parameter Z is given by

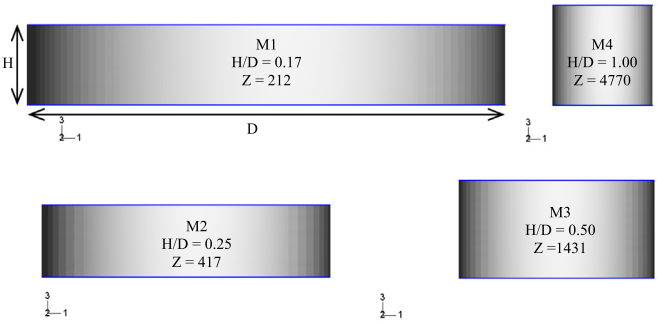

Fig. 13. Four cantilever cylinders considered as benchmark.

Table 4
Geometric properties of cantilever cylinders considered.

Model	Diameter	Height	Thickness	Non-dimensional parameters		
	D [m]	H [m]	t [mm]	H/D	R/t	Z
M1	24.0	4.0	6	0.17	2000	212
M2	14.0	3.5	6	0.25	1750	417
M3	9.0	4.5	5	0.50	1500	1431
M4	5.0	5.0	2	1.00	1250	4770

$$z = \frac{H^2}{Rt}\sqrt{(1-\nu^2)} \tag{29}$$

where H is the tank height, R is the tank radius, t the course thickness (assumed constant for this set of models) and ν is Poisson's ratio.

6.2. LBA and GNIA studies under wind pressure

This problem was originally solved in Ref. [51] and results of Ref. [48] are reported next. LBA studies using element STRI3 in ABAQUS yield eigenvalues λ^C=2.23 KPa for M1; λ^C=2.14 KPa for M2; λ^C=1.69 KPa for M3; and λ^C = 1.52 KPa for M4. As shown in Fig. 14, for the shortest shell with H/D=0.17 (identified as M1), GNIA results yield η=0.60. On the other hand, the tallest shell M4 with H/D=1, leads to η=0.95. Thus, significant variations in imperfection-sensitivity are to be reproduced by numerical studies using RSA and REA (Fig. 15)

Further, the results show significant differences in buckling mode as predicted by LBA and GNIA studies, and the two shapes are shown in Fig. 16 using the same normalized maximum amplitude of deflection.

6.3. Application of RSA

Based on experience using the methodology, results using RSA are shown next (Fig. 17) for two of the cases, M1 and M2. For M1, complete elimination of U^m leads to η=0.52 (13% lower than GNIA) which is a true lower bound; whereas if only U^m_{ss} or U^m_{ss} + U^m_{st} were eliminated, then an unacceptable value η=0.71 would be obtained. A similar situation is obtained for the other models M2 to M4 investigated.

As mentioned before, problems with RSA arise not in terms of buckling loads but in the context of the deflected shape at buckling. Take model M1 again, with full elimination of U^m, there are spurious modes with large amplitude displacements at θ=80°, which do not exist in GNIA. As said before, the application of RSA affecting just U^m at windward requires of a full two-dimensional element and is not possible to be done with semi-analytical formulations like ALREF or BOSOR.

This problem has been solved in the penalty formulation by adopting a value α less than 1, say 0.90, in which case the correct buckling mode is recovered without the presence of spurious modes. In conclusion, for wind loaded cantilever cylinders, the penalty approach allows computation of correct lower bounds with α=1, but if both eigenvectors and eigenmodes are needed, they should be computed α=0.9.

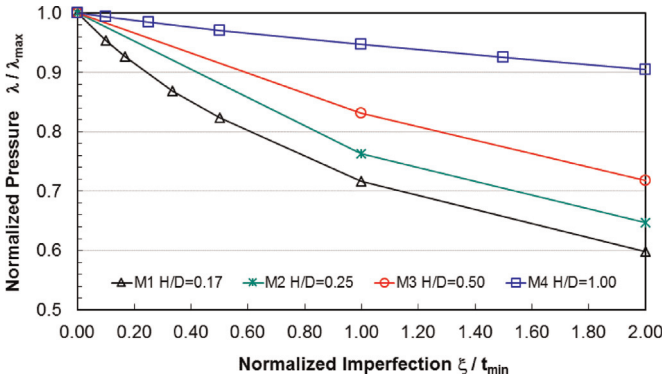

Fig. 15. Imperfection-sensitivity for all four cases M1–M4, using eigenvector-affine imperfection. Adapted from Ref. [48].

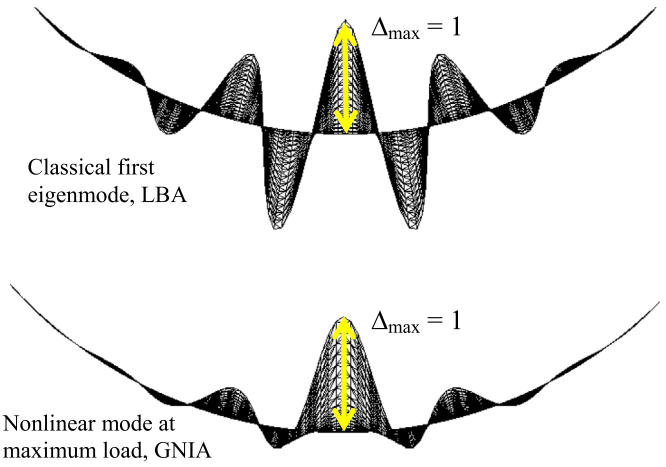

Fig. 16. Cantilever cylindrical shells under wind pressure. Differences in mode between LBA and GNIA studies for model M1.

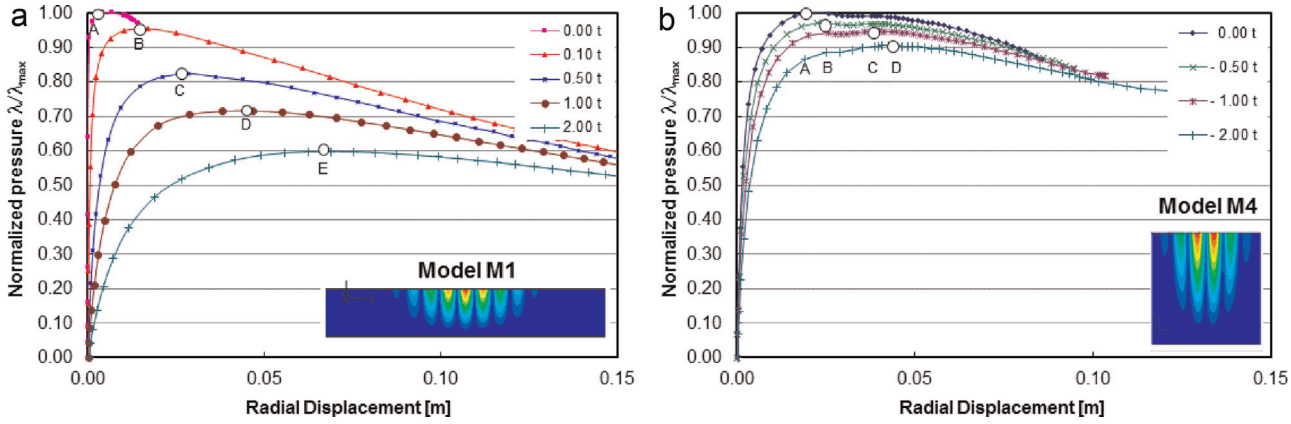

Fig. 14. Cantilever cylindrical shells under wind pressure, eigenmodes affine imperfection: first mode, GNIA results. Equilibrium paths (a) M1 (H/D=0.17); and (b) M4 (H/D=1.00).

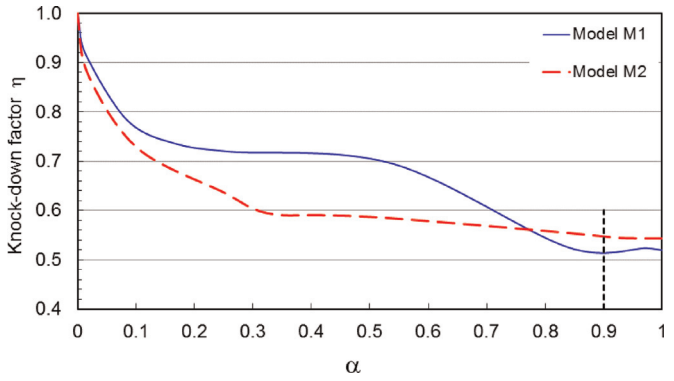

Fig. 17. Cantilever cylindrical shells under wind pressure, RSA results.

6.4. Application of REA

Use of REA as explained before in which mode preservation is assumed between LBA and GNIA, leads to conflicting results, as shown in Fig. 18. All imperfection sensitivity curves became almost identical, which is contrary to the GNIA results in which wild variations are obtained between M1 and M4.

The significant differences in η that should be expected from these quite different geometries (as reflected by GNIA) are not seen in the REA, in which all cases seem to be very close to each other. Because the modified eigenmode is not solved in REA, the classical mode is assumed to be valid in the lower bound analysis, which is not an adequate assumption in this case. Attention has been given to this point in Ref. [48], but the problem has not been solved yet.

7. Conclusions

New computational methodologies to implement lower bound buckling estimates for imperfection-sensitive shells using finite element analysis have been discussed in this paper. The methodologies reduce the membrane contribution in the classical eigenvalue problem by means of a penalty parameter and have been implemented in a special purpose finite element code via Reduced Stiffness, and in a general purpose finite element code via Reduced Energy Analysis. In all cases, the aim is to estimate lower bounds while at the same time adequately representing the buckling mode. Attention to this last point has not been given in previous research, and it emerges here because of the need to compute the correct mode shapes under wind pressures.

Some conclusions may be drawn as follows:

- REA and RSA are both based on the same philosophy, but employ different assumptions. In RSA the mode shape at the lower bound is not assumed, and it should be calculated by solving a modified eigenvalue problem. REA assumes that the lower bound mode is the same as in the classical eigenproblem. As employed in the literature, REA is a first-order analysis in a perturbation expansion, in which corrections to the classical eigenvector are not pursued.
- Both REA and RSA yield good lower bound estimates for buckling load under uniform pressure, for which the mode in the classical LBA is the same as in the reduced methodology.
- The use of RSA requires modification of a finite element code, and this can be achieved in special purpose codes, not in general purpose ones. This may become an obstacle to the adoption of this methodology in engineering practice.
- Modeling an isotropic metal shell as an orthotropic composite is a simple way to implement REA using a general purpose code.
- It has been shown that extension of RSA and REA to cases in which the mode changes between classical and lower bound solutions is not a simple task. Our results indicate that a REA implementation was not able to identify differences in imperfection-sensitivity benchmarks (cantilever cylinders under wind), for which there should be significant differences.
- The problems are less severe in RSA, with good estimates in lower bound buckling loads, but difficulties arise in the identification of the correct eigenvectors. Even with this limitation, the RSA can be implemented in special purpose finite element codes to estimate reasonably accurate know-down factors that could be acceptable in most applications.
- The region where the membrane stiffness should be degraded in the RSA is given by the first eigenmode computed in LBA. Under uniform pressure, the first eigenmode has periodic displacements on the entire shell, so that the stiffness degradation should affect the complete shell. Under wind the first eigenvector is dominated by displacements at windward, with the consequence that membrane degradation should be restricted to that region. Reducing the membrane contribution on the entire shell for wind load leads to a poor estimate of the RSA mode.
- A value of perturbation parameter $\alpha=1$ in RSA provides a true lower bound buckling load in all cases. Values of alpha smaller than 1 are to be employed only if one needs to obtain the correct eigenvector, i.e. the buckling mode associated with the lower bound.

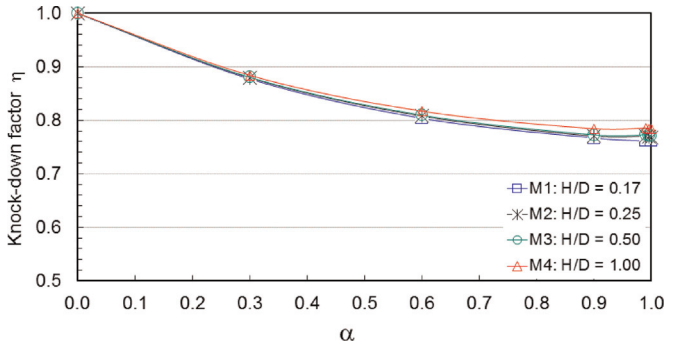

Fig. 18. REA results for tanks with open top and subjected to wind pressure.

Finally, a bias of the present lower bound approach is that it deals with deterministic imperfections. Other authors have investigated the influence of imperfections from a probabilistic perspective, notably Roorda [52] and Elishakoff [53,54], and the field has been brilliantly presented in book form in Ref. [55], but this is outside the scope of this paper.

Acknowledgments

This paper is dedicated to Prof. James G.A. Croll (Emeritus Prof., University College London, UK), who developed the lower bound methodology discussed in this work, and who guided us through many fruitful discussions and collaborative work in this field. LAG and FGF thank the support received through grants from the National University of Cordoba (SECYT-UNC) and CONICET (PIP 0126). RCJ thanks the support during this research received through grants from the National University of Comahue (SECYT-UNCo). LAG and FGF are members of the Research Staff of CONICET working at the Institute for Advanced Studies in Engineering and Technology.

References

[1] J.M. Rotter, H. Schmidt, Buckling of Steel Shells: European Design Recommendations, 5th edition,. European Convention for Constructional Steelwork (ECCS), Mem Martins, Lisbon, Portugal, 2008.
[2] W.T. Koiter, The stability of elastic equilibrium (Ph.D. thesis), Delft, The Netherlands, 1945.
[3] ASCE 7, Minimum Design Loads for Buildings and Other Structures, ASCE, Reston, VA, 2010.
[4] J.G.A. Croll, Towards simple estimates of shell buckling loads, Der Stahlbau 44 (1975) 243–248 (283–285).
[5] R.C. Batista, J.G.A. Croll, A design approach for unstiffened shells under external pressure, in: Proceedings of the International Conference on Thin Shell Structures, University of Strathclyde, Glasgow, UK, 1979.
[6] J.G.A. Croll, R.C. Batista, Explicit lower bounds for the buckling of axially loaded cylinders, Int. J. Mech. Sci. 23 (1981) 331–343.
[7] C.P. Ellinas, R.C. Batista, J.G.A. Croll, Overall buckling of stringer stiffened cylinders, Proc. Inst. Civil Eng. 71 (Part 2) (1981) 479–512.
[8] C.P. Ellinas, J.G.A. Croll, Experimental and theoretical correlations for elastic buckling of axially compressed stringer stiffened cylinders, J. Strain Anal. 18 (1) (1983) 41–67.
[9] C.P. Ellinas, J.G.A. Croll, Overall buckling of ring stiffened cylinders, Inst. Civil Eng. 71 (Part 2) (1981) 637–661.
[10] C.P. Ellinas, J.G.A. Croll, Experimental and theoretical correlations for elastic buckling of axially compressed ring stiffened cylinders, J. Strain Anal. 18 (2) (1983) 81–93.
[11] J.G.A. Croll, C.P. Ellinas, Reduced stiffness axial load buckling of cylinders, Int. J. Solids Struct. 19 (5) (1983) 461–477.
[12] G.M. Zintillis, J.G.A. Croll, Pressure buckling of end supported shells of revolution, Eng. Struct. 4 (1982) 222–232.
[13] G.M. Zintillis, J.G.A. Croll, Combined axial and pressure buckling of end supported shells of revolution, Eng. Struct. 5 (1983) 199–206.
[14] G.M. Zintillis, J.G.A. Croll, Pressure buckling of cantilever shells of revolution, Thin-Walled Struct. 4 (1986) 382–408.
[15] P.B. Goncalves, J.G.A. Croll, Axisymmetric buckling of pressure loaded spherical caps, ASCE J. Struct. Eng. 118 (4) (1992) 970–984.
[16] M. Kashani, J.G.A. Croll, Lower bounds for overall buckling of spherical space domes, ASCE J. Eng. Mech. 120 (5) (1994).
[17] M.D. Pandey, A.N. Sherbourne, Imperfection sensitivity of optimized laminated composite shells: a physical approach, Int. J. Solids Struct. 27 (1991) 1575–1595.
[18] J.G.A. Croll, Lower bound buckling loads for design of laminate composite cylinders, in: Proceedings of the International Conference on Buckling and Postbuckling Behavior of Composite Laminated Shell Structures, Braunschweig, Germany, March 25–27, 2015.
[19] S.G.P. Castro, R. Zimmermann, M.A. Arbeloa, R. Khakimovac, M.W. Hilburgerd, R. Degenhardt, Geometric imperfections and lower-bound methods used to calculate knock-down factors for axially compressed composite cylindrical shells, Thin-Walled Struct. 74 (2014) 118–132.
[20] C.P. Ellinas, J.G.A. Croll, Elasto-plastic general buckling of ring stiffened cylinders, in: J.M.T. Thompson, G.W. Hunt (Eds.), Collapse: The buckling of Structures in Theory and Practice, Cambridge University Press, Cambridge, UK, 1983, pp. 93–109.
[21] J.G.A. Croll, Lower bound elasto-plastic buckling of cylinders, Proc. Inst. Civil Eng. 71 (Part 2) (1981) 235–261.
[22] J.G.A. Croll, Elasto-plastic buckling of pressure and axial loaded cylinders, Proc. Inst. Civil Eng. 73 (Part 2) (1982) 633–652.
[23] J.G.A. Croll, C.P. Ellinas, A design formulation for axisymmetric collapse of stiffened and unstiffened cylinders, ASME J. Energy Resour. Technol. 107 (1985) 350–355.
[24] S. Yamada, J.G.A. Croll, Non-linear buckling response of pressure loaded cylindrical panels and its interpretation for design, Technol. Rep. Tohoku Univ. Jpn. 52 (2) (1988) 71–95.
[25] S. Yamada, J.G.A. Croll, Buckling behavior of pressure loaded cylindrical panels, ASCE J. Eng. Mech. 115 (2) (1989) 327–344.
[26] S. Yamada, J.G.A. Croll, Buckling and post-buckling characteristics of pressure loaded cylinders, ASME J. Appl. Mech. 60 (1993) 290–299.
[27] J.G.A. Croll, Towards a rationally based elastic–plastic shell buckling design methodology, Thin-Walled Struct. 23 (1995) 67–84.
[28] J.G.A. Croll, Stability in shells, Nonlinear Dyn. 43 (1–2) (2006) 17–28.
[29] D.O. Brush, B.O. Almroth, Buckling of Bars, Plates, and Shells, McGraw-Hill, New York, 1975.
[30] O.C. Zienkiewicz, R.L. Taylor, J.Z. Zhu, The Finite Element Method: Its Basis and Fundamentals, sixth edition,. Butterworth-Heinemann, Oxford, UK, 2005.
[31] J.M. Thompson, G.W. Hunt, A General Theory of Elastic Stability, Wiley, London, UK, 1973.
[32] L.A. Godoy, Theory of Elastic Stability: Analysis and Sensitivity, Taylor and Francis, New York, NY, 2000.
[33] R.E. Bellman, Perturbation Techniques in Mathematics, Physics and Engineering, Holt Rinehart & Winston, New York, NY, 1964.
[34] ABAQUS User's Manual, Documentation Collection Release 6.9, Dassault Systémes SIMULIA Corp., Providence, RI, 2009.
[35] ANSYS Academic Research, Release 16.0, ANSYS, Inc., Cecil Township, PA, 2009.
[36] F. Flores, L.A. Godoy, Elastic postbuckling analysis via finite element and perturbation techniques, Part I: formulation, Int. J. Numer. Methods Eng. 33 (1992) 1775–1794.
[37] E.M. Sosa, L.A. Godoy, J.G.A. Croll, Computation of lower bound buckling loads using general purpose finite element codes, Comput. Struct. 84 (29–30) (2006) 1934–1945.
[38] R.C. Jaca, L.A. Godoy, J.G.A. Croll, Reduced stiffness buckling analysis of aboveground storage tanks with thickness changes, Adv. Struct. Eng. 14 (3) (2011) 483–495.
[39] R.C. Jaca, L.A. Godoy, F.G. Flores, J.G.A. Croll, A reduced stiffness approach for the buckling of open cylindrical tanks under wind loads, Thin-Walled Struct. 45 (2007) 727–736.
[40] F.G. Flores, L.A. Godoy, Instability of shells of revolution using ALREF: studies for wind loaded shells, in: J.F. Jullien (Ed.), Buckling of Shells in Land, in the Sea and in the Air, Elsevier Applied Science, Oxford, UK, 1991, pp. 213–222.
[41] F.G. Flores, L.A. Godoy, Elastic postbuckling analysis via finite element and turbation techniques, Part II: application to shells of revolution, Int. J. Numer. Methods Eng. 36 (1992) 331–354.
[42] R. Jones, Mechanics of Composite Materials, 2nd ed., CRC Press, Boca Raton, FL, 1998.
[43] E.J. Barbero, Introduction to Composite Materials Design, second edition,. CRC Press, Boca Raton, FL, 2010.
[44] J.C. Virella, L.E. Suárez, L.A. Godoy, Impulsive modes of vibration of cylindrical tank-liquid systems under horizontal motion: effect of pre-stress states, J. Vib. Control 11 (9) (2005) 1195–1220.
[45] API Standard 650, Welded Steel Tanks for Oil Storage, American Petroleum Institute, Washington, DC, 2010.
[46] J.L. Batoz, K.J. Bathe, L.W. Ho, A study of three-node triangular plate bending elements, Int. J. Numer. Methods Eng. 15 (1980) 1771–1812.
[47] L.A. Godoy, Performance of storage tanks in oil facilities following hurricanes Katrina and Rita, ASCE J. Perform. Constr. Facil. 21 (6) (2007) 441–449.
[48] E.M. Sosa, L.A. Godoy, Challenges in the computation of lower-bound buckling loads for tanks under wind pressures, Thin-Walled Struct. 48 (2010) 935–945.
[49] D. Bushnell, BOSOR 5-Program for buckling of elastic–plastic complex shells of revolution including large deflections and creep, Comput. Struct. 6 (1976) 221–239.
[50] R.C. Jaca, L.A. Godoy, Computational strategies for lower bound buckling loads of wind loaded shells of revolution, in: Proceedings of the 10th World Congress on Computational Mechanics, Sao Paulo, Brazil, 2012.
[51] L.A. Godoy, F.G. Flores, Imperfection sensitivity to elastic buckling of wind loaded open cylindrical tanks, Int. J. Struct. Eng. Mech. 13 (5) (2002) 533–542.
[52] J. Roorda, Some statistical aspects of the buckling of imperfection-sensitivity in elastic post-buckling, J. Mech. Phys. Solids 17 (1969) 111–123.
[53] I. Elishakoff, How to introduce the imperfection-sensitivity concept into design, in: J.M.T. Thompson, G.W. Hunt (Eds.), Collapse: Buckling of Structures in Theory and Practice, Cambridge University Press, Cambridge, UK, 1983, pp. 345–357.
[54] I. Elishakoff, Probabilistic resolution of the twentieth century conundrum in elastic stability, Thin Walled Struct. 59 (2012) 35–57.
[55] I. Elishakoff, Resolution of the Twentieth Century Conundrum in Elastic Stability, World Scientific, London, 2014.